Characterization of the Absorbing Material Used in EMC Experiments

Zainul Ihsan, Grzegorz Lubkowski, Christian Adami, Michael Suhrke
Nuclear and Electromagnetic Effects
Fraunhofer INT
Euskirchen, Germany

***Abstract*—This paper deals with the modelling of the pyramid absorber wall commonly used in EMC experiments. The absorber material is characterized by coaxial line measurements in the frequency range from 20 MHz to 1.7 GHz. The electric permittivity of the material under test is extracted by Nicolson - Weir approach. The dielectric properties of the absorber are modelled by Debye formula and multilayer representation. Simulated results show that the content of the carbon loading the absorber foam is between 10% and 26%.**

***Index Terms*—TEM waveguide, pyramid absorber, coaxial line measurement, numerical field simulation**

I. Introduction

The transverse electromagnetic (TEM) waveguide gained a great interest in electromagnetic compatibility (EMC) tests where it is used e.g. to measure the immunity of a device under test (DUT) over a broadband frequency range. The geometry of an asymmetric, open, TEM waveguide consists of three metallic planes, where the input is connected to a signal generator and the output is terminated with an absorbing wall. The middle metal layer (called septum) is placed asymmetrically in the waveguide (relative height 0.77 in our case) to provide more space for the test volume (Fig. 1) [1].

Fig. 1. TEM waveguide for EMC tests in Fraunhofer INT

TEM waveguide is terminated by an absorber wall consisting of 0.94m long pyramids that suppress reflection of the incoming electromagnetic waves. The geometry of the pyramid and the complex permittivity of the absorbing material determine the ability to suppress the reflection in the high frequency band.

In order to model the absorber structure the dispersive characteristic of its electric permittivity is modelled by the Debye relaxation formula [2]. To identify the coefficients of the Debye model, the fraction of carbon in the absorber foam has to be assessed. If the carbon content in the absorber foam is not known, it can be approximated from measurements by relating the experimental results to the data available in the literature [3].

This paper is organized as follows. Section II presents the basic principles and results of the coaxial line measurement, Section III describes the results of the numerical analysis of the absorber geometry and finally Section IV closes the paper with conclusions and a brief outlook.

II. Coaxial Line Experiment

The coaxial line measurement is one of the non-resonant methods, where the sample under test is inserted into a segment of transmission line, and the permittivity and permeability of the sample are derived from the reflection and transmission of the sample-loaded unit [4]. In a coaxial line method, the toroidal sample of the material under test is inserted between the inner and outer conductors of the coaxial line. The advantage of this method is a wide frequency range (theoretically, it can work down to zero frequency). The main parameters of a coaxial line are its characteristic impedance and the working frequency range [4].

The coaxial line used in this work is made of brass with the inner and outer diameter of 8.5cm and 20cm, respectively (Fig.2). The line consists of two (inner/outer) cylinders forming the DUT section and corresponding cones connecting this section with the ports (Fig.3). The characteristic impedance of the air line determined by the outer/inner diameter ratio equal to 2.3 is $Z = 50\Omega$. Two styrofoam holders characterized by electric permittivity close to unity are used to ensure the mechanical stability of the structure. The length of the coaxial cylinder is 25cm, whereas input/output port distance is 75cm.

Theoretically, the working frequency range of the coaxial line is limited to 650 MHz (cutoff of the first higher order mode TE_{11} at 684 MHz). In practice, however, our coaxial line operates with a pure TEM mode up to the frequency of about 2.5 GHz, where the TE_{01} and TM_{01} modes start to propagate (see Fig.4) [5]. This was validated by the measurements of the coaxial air line. Providing that properly shaped, symmetrical probes of the tested material are used, it holds also for the measurements of the line loaded with the tested material.

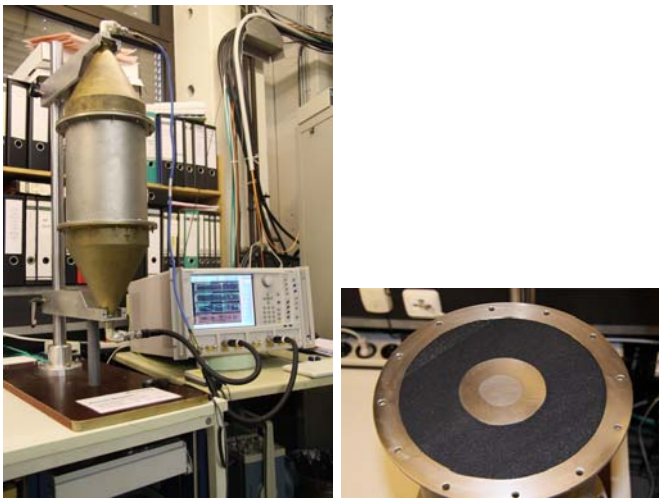

Fig. 2. LHS: The coaxial line setup, outer diameter of the DUT section 20cm; RHS: Absorber material under test fitted in the coaxial line

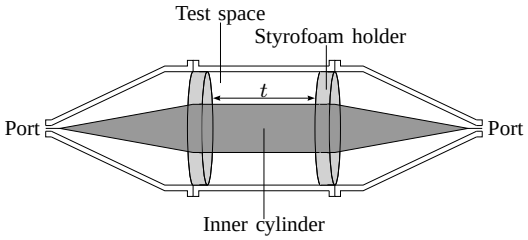

Fig. 3. The geometry of the coaxial line used in tests

The constitutive parameters of the material under test are derived from the measured S-parameters. The scattering matrix is measured with a vector network analyzer (Anritsu MS4644A) in the frequency range 20 MHz - 2.5 GHz corresponding to the working regime of the coaxial air line. For the DUT loaded line the higher order modes effects occur at the frequency of 1.8 GHz. Therefore, the frequency range of the valid results is limited to 1.7 GHz.

The S-parameters measured for the absorber probe are shown in Fig. 5. The measured magnitude of the transmission coefficient decays with the frequency due to the growing loss in the absorber material.

The S-parameters are converted to the electric permittivity of the material under test according to Nicolson-Weir algorithm [6]. First, the auxiliary variables V_1 and V_2 are calculated as:

$$V_1 = S_{21} + S_{11} \tag{1}$$

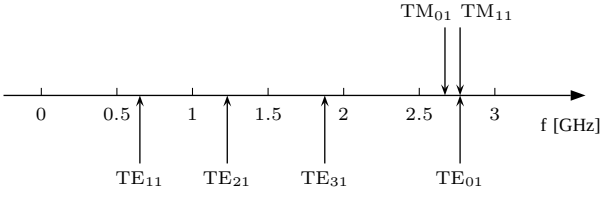

Fig. 4. Cutoff frequencies of the higher order modes in coaxial air line

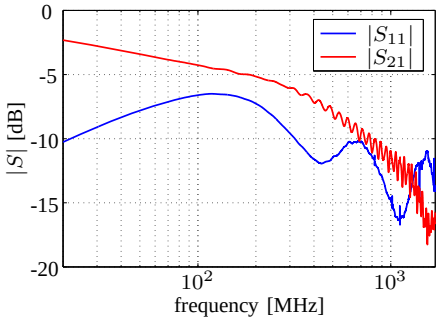

Fig. 5. The magnitude of transmission and reflection measured for the absorber sample

$$V_2 = S_{21} - S_{11} \tag{2}$$

These two expressions are used to calculate a variable X, denoted as:

$$X = \frac{1 - V_1 V_2}{V_1 - V_2} \tag{3}$$

whereas the reflection coefficient of a wave incident on the DUT interface is calculated as:

$$\Gamma = X \pm \sqrt{X^2 - 1} \tag{4}$$

where the appropriate sign is chosen in order to provide the fulfillment of the passivity requirement $|\Gamma| \leq 1$. In the next step the auxiliary variable z representing the transmission coefficient between faces of the DUT is computed as:

$$z = \frac{V_1 - \Gamma}{1 - V_1 \Gamma} \tag{5}$$

The relative electric permittivity of the material under test is finally expressed as:

$$\varepsilon_r = \varepsilon_r' - j\varepsilon_r'' = j\frac{1-\Gamma}{1+\Gamma}\frac{c}{\omega d}(\ln|z| + j(\arg(z) \pm 2\pi m)) \tag{6}$$

where ε_r' is related to the energy stored in the medium, ε_r'' accounts for loss in the medium, whereas ω, c and d are speed of light, angular frequency and thickness of the material probe, respectively. The variable $m = 0, 1, 2, \ldots$ is related to the phase ambiguity problem that is solved by phase-unwrapping method applied to z [4]. Fig. 6 shows the unwrapped argument of the z coefficient and the corresponding m values.

To verify the experimental setup and numerical procedure, the measurement of an empty coaxial line was performed that resulted in the expected value of unity for the extracted ε_r'. Fig. 7 shows the relative permittivity extracted from the measurements of the absorber sample in the frequency range 20 MHz - 1.7 GHz. As expected, the ε_r' characteristic decreases with frequency, from $\varepsilon_r' = 7.9$ at 20 MHz to $\varepsilon_r' = 1.9$ at 1.7 GHz [3], [7], [10]. The electric permittivity value equal to 1.9 at 1.7 GHz is in good agreement with the experimental observation of the starting frequency of the higher order modes occuring in the coaxial line. For empty line, this frequency equals $f_1 = 2.5$ GHz. For absorber loaded line it is $f_2 = 1.8$

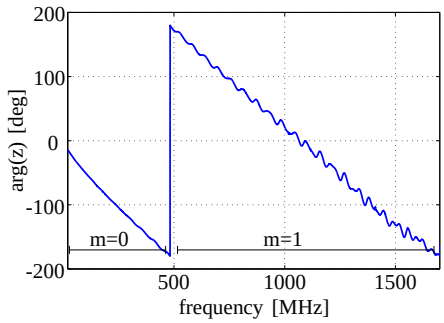

Fig. 6. The argument of z coefficient with the corresponding m values providing unwrapped phase characteristic

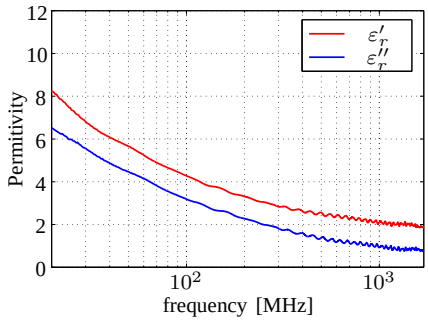

Fig. 7. Extracted electric permittivity for the absorber under test

GHz. As the cutoff frequency of higher order modes in a coaxial line scales as $f_2 = \frac{f_1}{\sqrt{\varepsilon'_r}}$ [8], the obtained $\varepsilon'_r = (\frac{2.5}{1.8})^2$ equals to 1.93 and is in good agreement with the extracted value $\varepsilon'_r = 1.9$.

III. Numerical Analysis of the Absorber Geometry

The dielectric material used in the fabrication of carbon loaded pyramid absorber can be modelled as a first-order dielectric with a static electric conductivity [2]. Permittivity of the absorber material can be represented by Debye equation [2]:

$$\varepsilon_r(\omega) = \left(\varepsilon_\infty + \frac{\varepsilon_s - \varepsilon_\infty}{1+\omega^2\tau_e^2}\right) - j\left(\frac{\sigma_e}{\omega\varepsilon_0} + \frac{(\varepsilon_s - \varepsilon_\infty)\omega\sigma_e}{1+\omega^2\tau_e^2}\right) \quad (7)$$

where ε_∞ is the optical relative permittivity, ε_s is the static relative permittivity, τ_e represents the dielectric relaxation time and σ_e is the electric conductivity. The coefficients of the Debye model for different carbon content ($7\%, 10\%, 26\%$ and 34%) are available e.g. in [2]. The dependence of the dispersive permittivity characteristic on carbon loading factor in the frequency range 20 MHz - 1 GHz is shown in Fig. 8.

The carbon content and the pyramid shape determine the reflectivity of the absorber. The pyramid acts as an impedance matching network, whereas the amount of carbon determines the effective characteristic impedance of the material [3]. As can be noticed from Fig. 8, larger carbon loading leads to

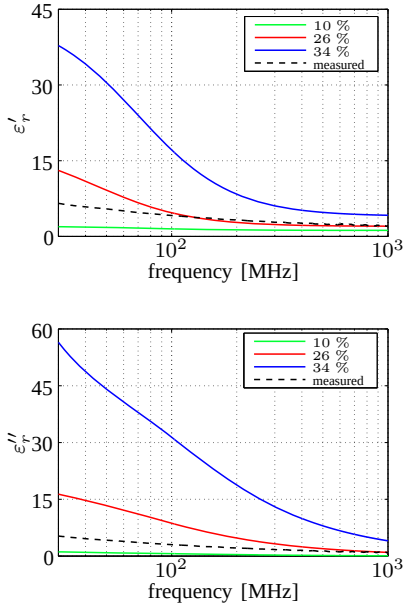

Fig. 8. Electric permittivity of the absorber material for different carbon contents compared with the experimentally obtained curves

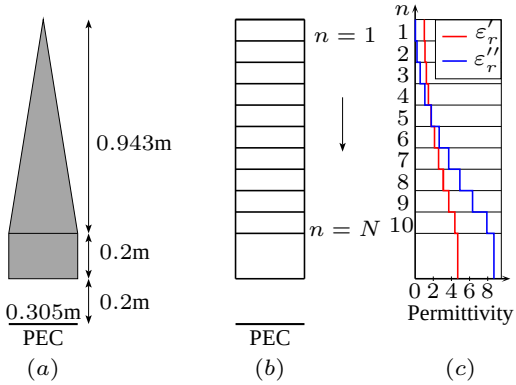

Fig. 9. (a) The geometry of the tested pyramid absorber; (b) Equivalent multilayer representation; (c) Electric permittivity profile at 100 MHz

larger values of ε' and ε''. The carbon content for the measured DUT is between 10% and 26%.

The investigated pyramid taper representing the absorber wall of the TEM waveguide is shown in Fig. 9a. The pyramid is modelled with a multilayer approach, by 10 planar layers parallel to the back wall of the cell (Fig. 9b) [9], [10], [11].

The effective permittivity of each layer is computed from the expression:

$$\varepsilon = g\varepsilon_a + (1-g)\varepsilon_0 \quad (8)$$

where g represents the fractional volume of the absorber, whereas ε_a and ε_0 are the electric permittivity of the absorber and free space, respectively. Consequently, the relative electric permittivity of each layer is derived as:

$$\varepsilon'_r(n) = 1 + g(n)(\varepsilon'_{ra} - 1) \quad (9)$$

$$\varepsilon''_r(n) = g(n)\varepsilon''_{ra} \quad (10)$$

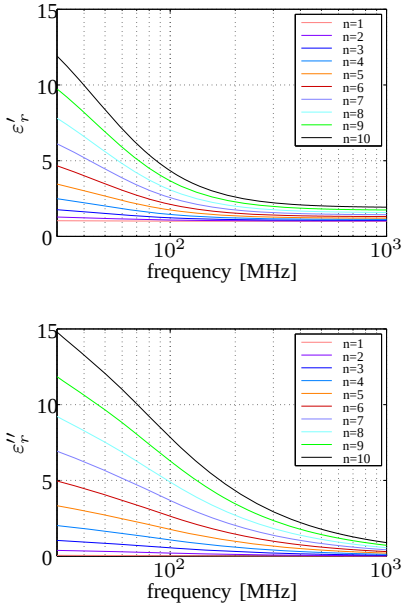

Fig. 10. Electric permittivity profiles for 10-layers absorber representation (26% carbon loading)

where $\varepsilon'_r(n)$ and $\varepsilon''_r(n)$ are the relative permittivity of the n-th layer (numbered from the top of the pyramid). The fraction volume of each layer $g(n)$ is expressed as:

$$g(n) = \frac{1}{3}\left(\frac{3n^2 - 3n + 1}{N^2}\right) \tag{11}$$

Fig. 9c shows the electric permittivity profile for 10-layer representation of the pyramid absorber characterized by 26% carbon loading. The $\varepsilon'_r(n)$ profile at 100 MHz starts at the value of $\varepsilon'_r(1) = 1.01$ and grows stepwise to $\varepsilon'_r(10) = 4.37$, whereas $\varepsilon''_r(n)$ starts at $\varepsilon''_r(1) = 0.03$ and grows to $\varepsilon''_r(10) = 7.91$ (cf Fig. 8).

The multilayer representation of the absorber material is valid for frequencies in the range 30 MHz - 1 GHz. The dispersive characteristics of the permittivity profiles for 26% carbon loading are shown in Fig. 10.

Three-dimensional full-wave simulation of the reflection from the pyramid model and its 10-layer representation results in a reasonable agreement, as shown in Fig. 11 (simulated with CST Microwave Studio [12]).

IV. Conclusion and Outlook

The measurement results of the dielectric properties of the absorber material have been presented. The absorber material has been measured in a coaxial line and its dielectric properties have been extracted by Nicolson - Weir approach in the frequency range 20 MHz - 1.7 GHz. The absorber material has been modelled by a Debye formula and by a multilayer effective representation. By comparison of the extracted electric permittivity with the data available in the referenced literature, the carbon loading factor for the material under test has been determined to be between 10% and 26%. The results obtained

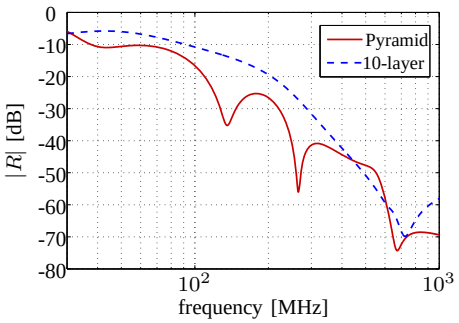

Fig. 11. Simulated reflection for TE wave incidence on 3D pyramid element described by Debye model (26% carbon loading) and its 10-layer effective representation

from 3D full-wave simulations of the pyramid geometry and its multilayer model showed a reasonable agreement in reflective properties of both structures.

Extension of the measured frequency range is planned in future work, by application of additional coaxial lines with different dimensions. The multilayer absorber model will be applied in the numerical analysis of the experimental TEM waveguide.

References

[1] H.U. Schmidt, *Die Messanlagen des INT fuer Feldeinkopplungsmessungen in Mikrowellenbereich*, International EMP Symposium IESM-91, Mannheim, 1991.

[2] J. Paul, *Modelling of general electromagnetic material properties in TLM*, PhD Thesis, University of Nottingham, 1998.

[3] C.L. Holloway, R.R. DeLyser, R.F. German, P. McKenna and M. Kanda, *Comparison of electromagnetic absorber used in anechoic and semi-anechoic chambers for emissions and immunity testing of digital devices*, IEEE Transactions on Electromagnetic Compatibility, Vol. 39, No. 1, pp 33-47, Feb 1997.

[4] L.F. Chen, C.K. Ong, C.P. Neo, V.V. Varadan and V.K. Varadan, *Microwave Electronics, Measurement and Materials Characterization*, John Wiley & Sons, 2004.

[5] N. Marcuvitz, *Waveguide Handbook*, IEE Press, 1986.

[6] A.M. Nicolson and G.F. Ross, *Measurement of the intrinsic properties of materials by time-domain techniques*, IEEE Transactions on Instrumentation and Measurement, Vol. IM-19, No. 4, pp 377-382, Nov 1970.

[7] R.R. DeLyser, C.L. Holloway, R.T. Johnk, A.R. Ondrejka and M. Kanda, *Figure of merit for low frequency anechoic chambers based on absorber reflection coefficients*, IEEE Transactions on Electromagnetic Compatibility, Vol. 38, No. 4, pp 576-584, Nov 1996.

[8] D.M. Pozar, *Microwave Engineering*, 3rd ed., John Wiley & Sons, 2005.

[9] E.F. Kuester and C.L. Holloway, *A low-frequency model for wedge or pyramid absorber arrays-I: Theory*, IEEE Transactions on Electromagnetic Compatibility, Vol. 36, No. 4, pp. 300-306, Nov 1994.

[10] C.L. Holloway and E.F. Kuester, *A low-frequency model for wedge or pyramid absorber arrays-II: Computed and Measured Results*, IEEE Transactions on Electromagnetic Compatibility, Vol. 36, No. 4, pp. 307-313, Nov 1994.

[11] M. Al-Hamid, S. Schulze, R. Vick and M. Leone, *Validation of the MoM simulation model for GTEM including pyramid absorber*, Proceedings of the EMC Europe 2010, Wroclaw, pp. 603-608, 13-17 Sep 2010.

[12] CST Microwave Studio 2010. http://www.cst.com